Sinusoidal and Delta Function Responses of Visual Cells of the *Limulus* Eye

R. B. PINTER

From the Department of Electrical Engineering, Technological Institute, Northwestern University, Evanston, Illinois, and the Department of Electrical Engineering, University of Washington, Seattle, Washington. Dr. Pinter's present address is the Department of Electrical Engineering, University of Washington, Seattle, Washington

ABSTRACT Dynamic responses of visual cells of the *Limulus* eye to stimuli of sinusoids and narrow pulses of light superimposed on a nonzero mean level have been obtained. Amplitudes and phase angles of averaged sinusoidal generator potential are plotted with respect to frequency of intensity modulation for different mean levels of light adaptation. At frequencies above 10 CPS, generator potential amplitudes decrease sharply and phase lag angle increases. At frequencies below 1 CPS, amplitude decreases. A maximum of amplitude in the region of 1 to 2 CPS is apparent with increased mean intensity. The generator potential responses are compared with those of differential equation models. Variation of gain with mean intensity for incremental stimuli is consistent with logarithmic sensitivity of the photoreceptor. Frequency response of the photoreceptor derived from narrow pulses of light predicts the frequency response obtained with sinusoidal stimuli, and the photoreceptor is linear for small signals in the light-adapted state.

The logarithmic steady-state response of the *Limulus* ommatidium to step functions of light intensity has long been a subject of experiment and discussion. The dynamic or time-varying properties of this same response have not received as much attention as the steady state, and only recently have important analyses of these dynamic properties been published (Fuortes and Poggio, 1963; Fuortes and Hodgkin, 1964; Ratliff et al., 1963).

The dynamic characteristics of the generator potential of the *Limulus* ommatidium are nonlinear in three important respects. First, in response to steps of light, per cent peak overshoot[1] of the initial peak of the generator

[1] Defined as $\frac{\text{peak magnitude} - \text{steady-state magnitude}}{\text{steady-state magnitude}}$

potential varies with the intensity of the light step. Regardless of its form, variation of per cent peak overshoot with input intensity implies that the system under study is nonlinear. Second, in *Limulus* the variation of per cent peak overshoot is a nonlinear function of intensity of light step, in that per cent peak overshoot first increases with increasing intensity of light step, and then decreases with further increase of intensity of step. Third, the response to the "off step" of light is always monotonic with no peaking, for short times (1 sec). In contrast, a linear system would possess a response to the off step which is the exact inverse of that of the "on step." These nonlinear properties are evident in the records of Fuortes (1958) and Fuortes and Poggio (1963). They are evident to a lesser degree in records of nerve impulse activity in the single fiber (Hartline, 1935).

Considering the *Limulus* photoreceptor as a nonlinear dynamic system, with an input of light intensity and an output of generator potential, the above properties suggest that the damping of the natural frequencies of this dynamic system is decreasing with greater intensity of the light step, but that this decrease is limited at high intensities. In other words, the high frequency gain of the dynamic system increases with light intensity with a limit. This may also be inferred from Fig. 12 of Fuortes and Hodgkin (1964), where responses to flashes of light under dark- and light-adapted conditions are compared.

It is logical then to examine the changes of natural frequencies with respect to light intensity in this nonlinear dynamic system by means of sinusoidal variations of light intensity superimposed on a mean level to which the photoreceptor is adapted. If the system possesses linearity for small variations of light intensity about a mean level, a Bode plot can be drawn for that mean level. In contrast to large steps of light intensity, this type of analysis is a better method of finding parameters, since those parameters depending on the state of adaptation are held constant.

The validity of the small signal frequency response description of *any* nonlinear system, including the *Limulus* photoreceptor, might not exist for other than sinusoidal variations in the input. Given a nonlinear system for which only the small signal frequency response has been obtained, the response of this system to time waveforms other than sinusoids cannot be safely predicted by Fourier methods until the response to these other waveforms has been experimentally established. For example, a system, such as the pupillary reflex (Clynes, 1961), may have a rate-sensitive element which is not apparent in sinusoidal responses, but which yields remarkably different responses for small signal square pulse inputs than would be predicted from Fourier analysis of sinusoidal responses alone. Thus, the derivation of the frequency response of the generator potential from other time waveforms of light intensity is necessary. Fourier components of generator potential responses to

approximate delta functions of light intensity are compared with frequency response in this article.

The dynamic system under discussion presumably results from time delays present within and interactions among the systems of chemical kinetics of rhodopsin breakdown, transmitter substance generation, and eccentric cell membrane resistance variation. However, the degree of contribution to the over-all dynamics of each of these component systems cannot be directly deduced from input-output relationships such as those presented here.

METHODS

For these experiments, *Limulus* were obtained from Woods Hole, Massachusetts, and kept in tanks of cooled artificial sea water. The lateral eye was sectioned in two using a microtome while the eye was held in a stainless steel clamp. The eye was then placed in an artificial sea water of the same composition as that used by Benolken (1959). In all experiments the temperature was held at 18°C by means of a regulating system.

Micropipettes filled with 2 M KCl and having a resistance in the range of 40 to 100 megohms when placed in the artificial sea water were held in a micromanipulator. The micropipette was lowered approximately 1 μ at a time into one of the exposed ommatidia. If the peak of a generator potential response was in the range +40 to +90 mv relative to the resting potential in response to an intense step of light, the preparation was allowed to dark adapt and a control response was established.

The micropipette was connected to a neutralized input capacity electrometer tube amplifier (Bioelectric Instruments DS2B) by means of a Ag-AgCl electrode. The output from this amplifier was fed to an oscilloscope (Tektronix 502), and the output from this oscilloscope's DC vertical amplifier was fed to an FM tape recorder, or in some experiments, directly to the input of an averaging computer. The readout of the averaging computer and, in one case, of the tape recorder was recorded on an ink writing pen recorder. Except for one case as noted in the Results, the bandpass of the complete amplifying and recording system exceeded 3 db down at 1000 CPS which was sufficient for this work. The highest frequency of interest present in the generator potential was normally 25 CPS.

The use of small signal sinusoidal and delta functions of light intensity and the presence of noise on the generator potential made it necessary to employ averaging methods. The mathematical details of the reduction of variance of the average response as compared with the samples for additive signal and random noise have been worked out by Geisler (1960). In some experiments, repeated averages of responses were made and the average responses were found to be repeatable. In this work, both a Nuclear Data ND-800 Digital Memory Oscilloscope and a CAT 400B averaging computer were used. The sweep of the averaging computer was synchronized with the stimulus waveform by means of trigger pulses derived from the stimulus.

For the experiment of Figs. 1 through 8, and 14, a two channel optical system employing beam splitters and polaroids was used. This system provides a sum of a sinusoidally modulated light intensity and an unmodulated light intensity, and is based on the design of Kelly (1961 *a*). The rotating polaroid was driven by an adjust-

able speed DC motor and an adjustable speed mechanical transmission to give the necessary frequency range. The light source was a 100 w zirconium arc lamp (Sylvania C100P) driven with a regulated and monitored power supply. The passage of light through the beam splitter and polaroid system was confined by means of stops, and the exit ray was directed upon a facet of the *Limulus* eye by means of a f1.4 photographic objective lens. The resultant spot on the eye was approximately 80 μ in diameter, in order to confine illumination to one ommatidium. The light intensity waveform entering this lens was monitored with a photomultiplier tube and oscilloscope.

The light output from the polaroid-beam splitter system possesses a constant angle of polarization determined by the angle of the final fixed polaroid. This polaroid is adjustable, however, and is used to set the percentage modulation. In this work, percentage modulation M of the light intensity waveform is defined as

$$M = \frac{\frac{1}{2} \text{ peak to peak intensity of sine wave}}{\text{average intensity}} \times 100$$

and varies from 0 to 100%. A feature of this system is that the average intensity of the light remains nearly constant (variation less than 4% of maximum intensity) as the percentage modulation is adjusted from 0 to 95% by turning the final polaroid. In turning the final polaroid the angle of polarization of the light on the eye is changed. In a control experiment using a light source and one polaroid, however, it was found that this angle of polarization had no measurable effect on photoreceptor response. Further, sinusoidal and step function photoreceptor responses and responses due to changing percentage modulation were examined with a system (described below) which does not polarize the light, and were found to be similar to responses using the polarizing system.

In all experiments only ommatidia which were nearly in the horizontal plane were used. Further, the eye holder was rotated in the horizontal plane under the microscope so that the optic axis of the ommatidium was as close as possible to the horizontal plane optic axis of the final lens. These adjustments were made before probing with the micropipette, and yielded maximally sensitive preparations. A further effect of this alignment was to minimize sensitivity of the ommatidium to polarized light.

The usual spectral shift toward short wavelengths apparent when polaroids are crossed is not apparent in this system, since the maximum intensity of this "violet light" at complete crossing of the modulating polaroids is 0.005% of the average intensity, using polaroid specifications. The sinusoidal waveform generated by this system has a 120 CPS ripple of 10% of the average intensity, due to the arc lamp, but since the generator potential response to a sinusoid of light intensity is attenuated by at least a factor of 100 at 30 CPS, and is attenuated further at higher frequencies (by a factor of 4×10^5 at 120 CPS by extrapolation of Fig. 2), this ripple should not be an important factor in obtaining these results. The sinusoidal waveform has a further distortion of approximately 5% of peak to peak intensity, due to slight rounding of the minimum. This did not appear to cause any artifact in view of results obtained with the system described below.

Light intensity waveforms for Figs. 9 through 13 were produced by means of a

controlled current output driver unit exciting a Sylvania R1130B glow modulator tube. The driver unit output current is linearly proportional to its input voltage. In order to obtain a linear relationship of light intensity output to current through the glow tube, an orange-linearizing color filter must be used, in this case an Ilford 808 (Wratten No. 22). The frequency response of light intensity output to input voltage of the glow tube driver was flat to 35 CPS, and a ten turn potentiometer was used to set intensities and percentage modulation. The orange spectral characteristic of this stimulus did not appear to affect the transient or sinusoidal responses of the generator potential. The same lens and photomultiplier monitor as in the polaroid system were used, with approximately the same spot size on the *Limulus* eye.

In both systems the light passed through 5 cm of water in an optical cell before reaching the eye. Stray light was prevented from reaching the eye by a light-tight cage, shielding of the optical system, and subdued room light. Light intensity figures given in the text were obtained by photometry of the converging cone of light leaving the lens using an SEI (Salford Electrical Industries, Salford, England) hand photometer.

RESULTS

A. *High Frequency Sinusoidal Stimuli*

Fig. 1 shows a set of typical waveforms of averaged generator potentials in response to a sinusoidally modulated light intensity of percentage modulation 30%. The "bumps" of records *B* and *C* which represent departures from a sinusoidal waveform are due to attenuated action potentials present on the recorded generator potential. These action potentials are presumably conducted decrementally from a more proximal locus in the ommatidium, and were present in all experiments. All the generator potentials recorded in these experiments are thus in the large generator potential–small action potential category (MacNichol, 1956). Amplitude and phase for the Bode plots were obtained by measurement on records such as those of Fig. 1. Record *F* of Fig. 1 shows the distortion typical of the generator potential at high percentage modulations and frequencies of 1 CPS or less. The distortion consists of the rising portion of the wave being faster and the falling portion being slower than a pure sinusoid of the same period. In all cases the preparation is completely light-adapted to the mean intensity of the sinusoidal input.

In the Bode plot of generator potential obtained from averaged responses shown in Figs. 2 and 3 there are several notable features. Since percentage modulation is constant with decreasing mean light intensity levels, the incremental gain of the photoreceptor is increasing with decreased mean intensity levels. Incremental gain of the photoreceptor will be defined, in the usual sense, as

$$\text{Incremental gain} = \frac{\text{peak to peak generator potential, mv}}{\text{peak to peak light intensity, relative units}}$$

Changes of incremental gain are demonstrated in Fig. 4, in which the incremental gain of the photoreceptor has been plotted at 1 CPS with respect to mean light intensity of the stimulus. For a purely logarithmic sensitivity, i.e.

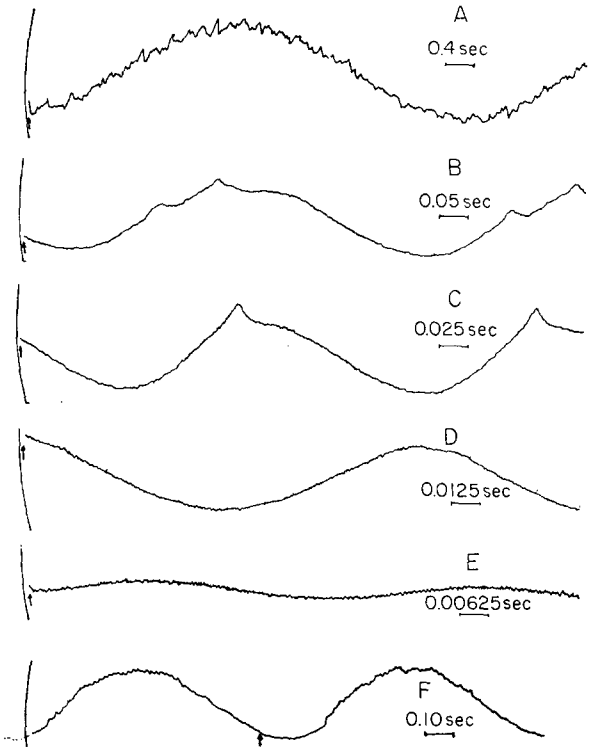

FIGURE 1. Records *A* through *E*, typical waveforms of averaged generator potential in response to sinusoidal light intensity. Vertical scales are arbitrary, and curvilinear. Frequencies, *A*, 0.16 CPS; *B*, 1.6 CPS; *C*, 3.9 CPS; *D*, 5.8 CPS; *E*, 13.5 CPS. Sample size in *A* is 8; *B*, 37; *C*, 53; *D*, 121; *E*, 339. Bumps on *B* and *C* are due to spikes on generator potential, presumably conducted to electrode site from proximal end of ommatidium. 30% modulation on mean intensity of approximately 13,600 lumens/m^2. Upward arrow at left end of each record indicates position of the minimum of sinusoidal intensity modulation. Increase of phase lag with increased frequency is thus indicated by shift of averaged response waveform to the right in records *A* to *E*. Record *F*, generator potential (not averaged) in response to 95% modulation, 1.1 CPS, mean intensity 136,000 lumens/m^2. Upward arrow near center of record indicates minimum of sinusoidal intensity modulation.

generator potential depends on the logarithm of light intensity in the steady state, the gain of the photoreceptor for incremental light intensity stimuli will be a 45° line on an equal axis log-log plot, which is shown on Fig. 4 as the solid line. The gain of the photoreceptor derived from sinusoidal incremental light intensity stimuli falls near this 45° line, which confirms an approximate

logarithmic sensitivity for incremental stimuli. In addition, the incremental gain of the photoreceptor has been calculated graphically by taking the first derivative of the static generator potential vs. light intensity curve for the same preparation, and plotted on Fig. 4.

The incremental gain of an initially dark-adapted photoreceptor decreases with time during stimulation by light of constant intensity, until a steady state is reached (unpublished observations of the author). This steady state is

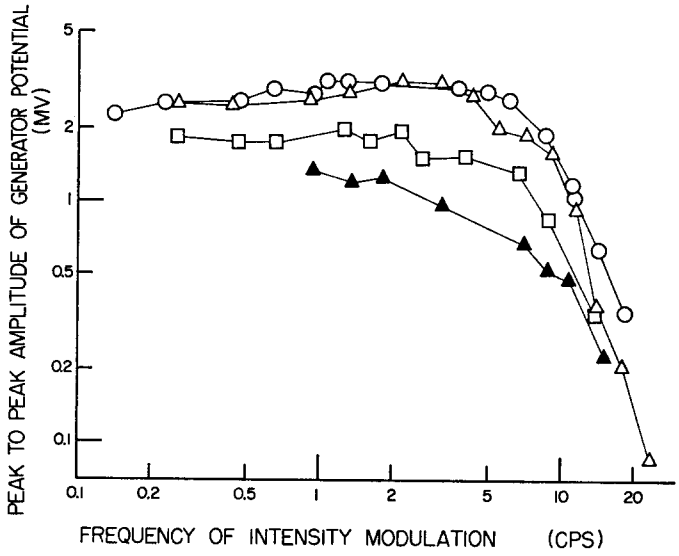

FIGURE 2. Generator potential sinusoidal response amplitude characteristics for different mean intensities to which the photoreceptor is adapted. Amplitudes obtained from averaged responses, sample size typically that of Fig. 1. ○, mean intensity 13,600 lumens/m²; △, mean intensity 1710 lumens/m²; □, mean intensity 136 lumens/m²; ▲, mean intensity 13.6 lumens/m²; all at percentage modulation 40%. Experiment of 14 November 1963.

coincident with a state of complete light adaptation at that intensity. Thus, the fact that in Fig. 4 the incremental gain of the photoreceptor obtained from sinusoidal stimuli is consistently higher than the incremental gain obtained from the first derivative of the static characteristic cannot be explained on the basis of differing states of light adaptation in the two cases. Measurement of the sinusoidal responses was made in a state of complete light adaptation, while the measurement of static generator potential was made 4 sec after onset of step. On the other hand, the incremental gain obtained from the first derivative of the static characteristic is a measurement made at zero frequency, whereas the sinusoidal measurements were made at 1 CPS. The Bode plots of generator potential (Fig. 2) show increased attenuation at lower

frequencies, and thus it might be expected that incremental gain at zero frequency would be less than incremental gain at 1 CPS.

The fact that the time constants of the photoreceptor gain increase with a decreased level of light adaptation is also demonstrated in Fig. 2. The amplitude of the generator potential in the range 2 to 8 CPS relative to the amplitude at 1 CPS decreases at the lower mean intensities. This is implied in the large signal step responses, as previously discussed. The high frequency asymptote of each of the amplitude characteristics of Fig. 2 is approximately 36 db per

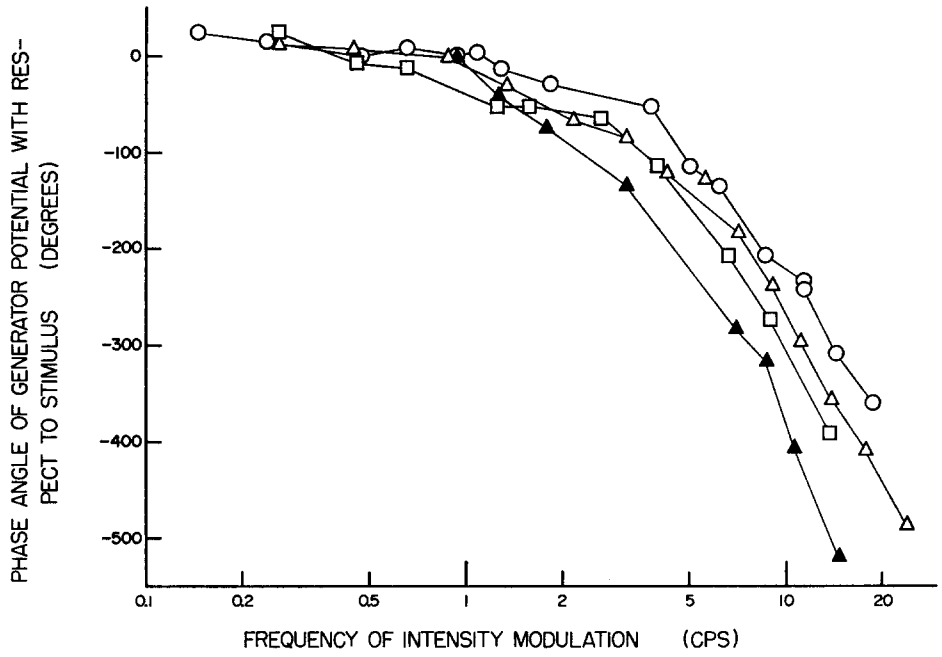

FIGURE 3. Generator potential sinusoidal phase angle characteristics corresponding to amplitude characteristics of Fig. 2. Negative phase angle means generator potential lagging stimulus. ○, mean intensity 13,600 lumens/m²; △, mean intensity 1710 lumens/m²; □, mean intensity 136 lumens/m²; ▲, mean intensity 13.6 lumens/m²; all at percentage modulation 40%. Experiment of 14 November 1963.

octave of frequency, which fact requires that the differential equation describing such a process be of at least 6th order. In other words, the RC model as used by Fuortes and Hodgkin (1964) would need at least 6 sections. However, the data of Fig. 2 do not preclude the model containing more than 6 sections, since data points for frequencies higher than those obtained, if they existed, might yield a steeper high frequency asymptote than 36 db per octave. The probability that such data points would yield a less steep asymptote is small.

In obtaining the high frequency asymptote of any noisy system, a problem

of number of averages required to detect signal in noise is encountered. In an experiment such as this, where the response is obtained at a constant rate in time, i.e., a constant number of responses per second, the averaging time required to increase the signal to noise ratio to a fixed value increases approxi-

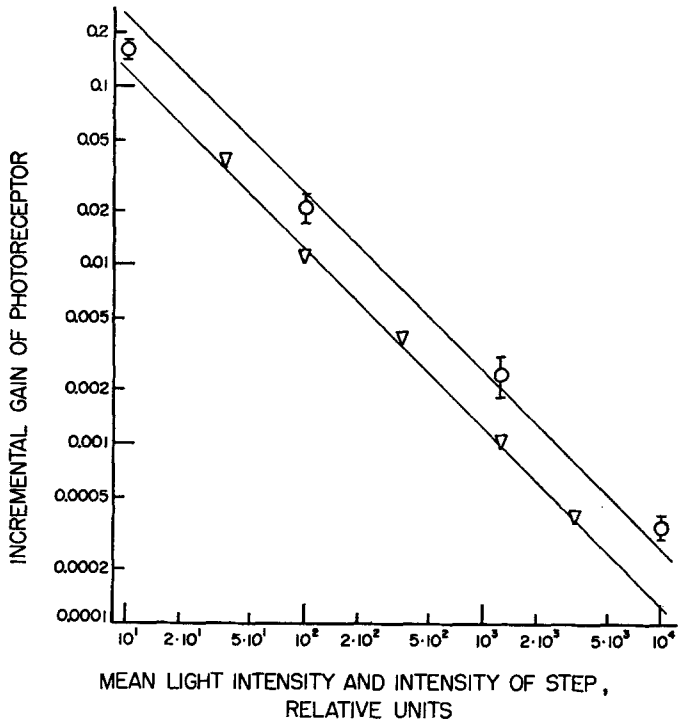

FIGURE 4. Incremental gain of the photoreceptor (defined in text). O, incremental gain computed for 70, 54, 40, 24, 13, and 4.6% sinusoidal modulation of the mean intensity on the abscissa, frequency approximately 1 CPS, bars indicate standard deviations. ▽, incremental gain at zero frequency computed by taking first derivative of graph of depolarization of eccentric cell vs intensity of large step. Intensity of step for each calculation is on the abscissa. Solid lines, incremental gain $\frac{\Delta y}{\Delta x}$ of function $y = a \log_{10} x$, fitted by inspection to experimental points, where a has two values, the uppermost line corresponding to $a = 5.76$, the lower to $a = 2.77$. 10^4 relative units equivalent to 13,600 lumens/m^2. Experiment of 14 November 1963.

mately as the 12th power of the stimulus frequency, assuming a 36 db/octave asymptote. This figure assumes additive Gaussian noise and signal, which is probably not completely true for the photoreceptor. Types of signal and noise mixing other than addition would not yield a smaller averaging time.

The measurements of phase angle of generator potential response with respect to stimulus corresponding to the amplitudes of Fig. 2 are shown in Fig.

3, and show an increase of phase angle lag with a decrease in gain, as frequency is raised. This is a property normally found in linear physical systems. Below 0.6 CPS the phase angle becomes leading; i.e., the phase of the generator potential leads the phase of the stimulus. This phase lead can be interpreted in terms of an adaptation of the generator potential at low frequencies, which is discussed later (Fig. 9).

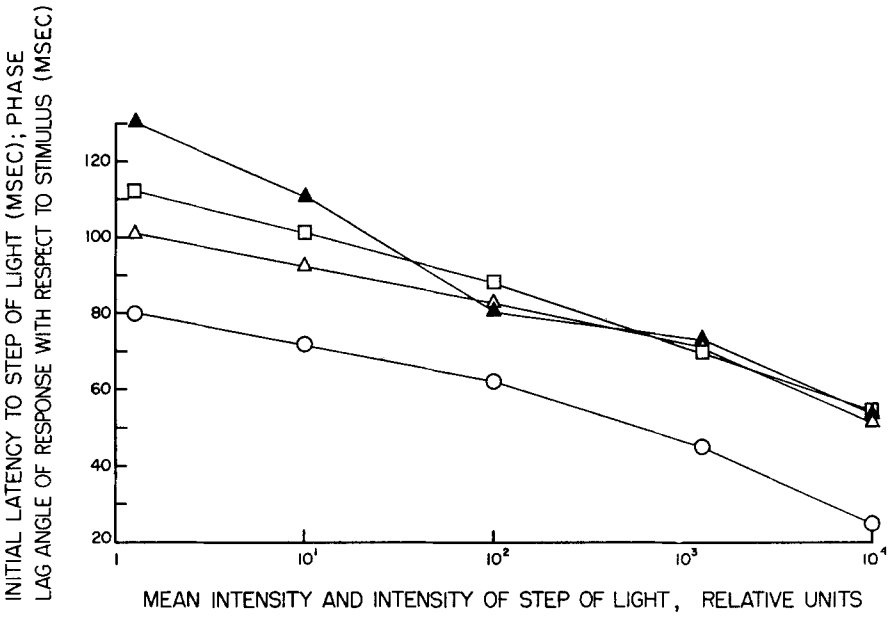

FIGURE 5. Comparison of initial latency of generator potential response to a step of light from dark-adapted state with phase lag (in milliseconds) of sinusoidal generator potential response with respect to stimulus. ○, initial latency to step of light of magnitude on the abscissa. ▲, phase lag of generator potential, in milliseconds, for sinusoidal stimulus frequency of 6.0 CPS. □, phase lag of generator potential for 10.0 CPS. △, phase lag of generator potential for 13.5 CPS. All sinusoidal responses are for 40% sinusoidal modulation on a mean level given by abscissa. 10^4 relative units equivalent of 13,600 lumens/m^2. Latencies measured as time from onset of stimulus to response rising out of noise. Experiment of 14 November 1963.

The increased phase lag of the generator potential (especially noticeable at higher frequencies) at decreased levels of mean intensity is predicted from the sinusoidal amplitude characteristics (Fig. 2) and the latency of response to steps of light intensity in the following qualitative way. With a decrease in step intensity, the initial latency of the generator potential response to the step of light intensity from the dark-adapted state becomes longer, as shown in Fig. 5. This fact alone may predict an increased phase lag at lower mean intensities for sinusoidal stimuli, and the phase lag in milliseconds is plotted

on Fig. 5 for three frequencies. The sinusoidal phase lag curve is similar to the step latency curve, suggesting that the increased latency is contributing to the increased phase lag. However, the dynamic system giving rise to the generator potential consists also of elements causing the amplitude attenuation (Fig. 2), and the amplitude characteristics increase in attenuation at decreased mean intensity levels. A further increase in phase lag over that caused by the latency is required by linear system theory due to the increased attenuation, and this causes the sinusoidal phase lag to be greater than that due to the latency alone, the deviation being the largest for the lowest mean intensities.

The initial latency to steps of light intensity from the dark-adapted state might not contribute at all to a latency for incremental stimuli around a mean level to which the photoreceptor is completely light-adapted. However, in one experiment the latencies of responses to incremental pulses of light at three mean levels were compared with the latencies to large steps (from the dark-adapted state) of the same magnitudes as the mean levels. In each case the latency was measured as the time to the point at which the response rises from the noise, and in each case the latencies were approximately the same. There appears to be no a priori reason for this equivalence.

B. *Comparison of Sinusoidal Data to Fuortes-Hodgkin Model*

It is not necessary to separate the dynamic system yielding the generator potential into two parts, one a latency giving phase lag but no attenuation, and the other giving both attenuation and phase lag. The model of Fuortes and Hodgkin (1964) which possesses the correct quantitative initial step and complete pulse response properties, will account in a qualitative way for these sinusoidal responses. This model has a latency which is not a true transport lag, but which is a time lag due to the large number of RC sections, each of which is described by equation (1)

$$\frac{dV_i}{dt} = \frac{V_{i-1}}{C} - \frac{V_i}{C}(g_o + aV_o) \qquad (1)$$

For purpose of comparison to sinusoidal data here, these equations were solved on a Pace (Electronics Associates, Inc., Long Branch, N.J.) analog computer. For the curves of Figs. 6 and 7 this model consisted of 9 sections, where $i = 2, \cdots 10$ and $V_1 = I$, the input light intensity, and $V_{10} = V_0$, the output, which can be thought of as the generator potential. V_{10} is to be thought of as a variable which immediately precedes generator potential, since generator potential itself would probably not affect the gain of preceding elements or membrane conductance (Fuortes and Hodgkin, 1964).

The amplitude and phase characteristics of Figs. 6 and 7 are qualitatively

similar to those of Figs. 2 and 3. However, the peaking in the sinusoidal amplitude characteristic of the RC model is more pronounced than in Fig. 2. For purposes of comparison, the highest and lowest mean level experimental sinusoidal characteristics are plotted on Figs. 6 and 7, using the best fit by inspection of the highest mean sinusoidal intensity, 13,600 lumens/m², as a

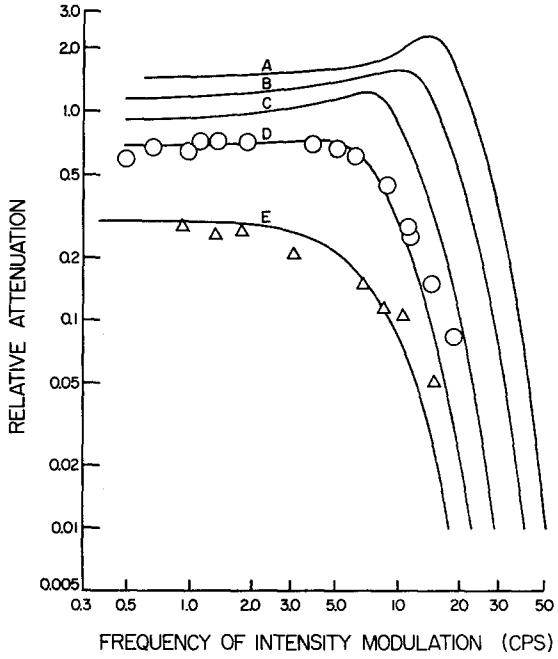

FIGURE 6. Comparison of small-signal sinusoidal frequency response characteristics of equation (1) with experimental results of Fig. 2. Solid curve *A*, amplitude characteristic of V_o of equation (1) where V_1 is a sinusoid imposed on a 95 v (analog computer) mean level, 10% modulation. Curve *B*, mean level 10 v, 20% modulation. Curve *C*, mean level 1 v, 20% modulation. Curve *D*, mean level, 0.11 v, 20% modulation. Curve *E*, approximately zero mean level; i.e., frequency response of V_o of equation (1) where $aV_o \ll g_o$. ○, amplitude characteristic from Fig. 2, mean intensity 13,600 lumens/m². △, amplitude characteristic from Fig. 2, mean intensity 13.6 lumens/m². Parameter values of equation (1) in computer time: $\frac{1}{C} = 7.0$, $g_o = \frac{1}{2}$, $a = \frac{1}{10}$. (Computer time) × 0.033 = (real time).

starting point. In other words, a time transformation between the experimental and the analog computer data is established by the best fit by inspection of the 13,600 lumen/m² amplitude–frequency response points to the analog computer simulation, and all other points are plotted by means of this transformation. The results are then plotted on the real time (frequency) scale. The transformation of computed curves to the real time scale is (com-

puter time) × 0.033 = (real time). The amplitude characteristics are arbitrarily placed on the vertical scale.

In Figs. 6 and 7 comparisons are being made between amplitudes of undistorted sine waves. For small amplitude sinusoidal inputs, equation (1) has undistorted sinusoidal output, but the feedback loops present from the output V_o to each RC section cause amplitude response peaking, seen in Fig. 6. This is so because equation (1) is not a simple cascade of RC elements for

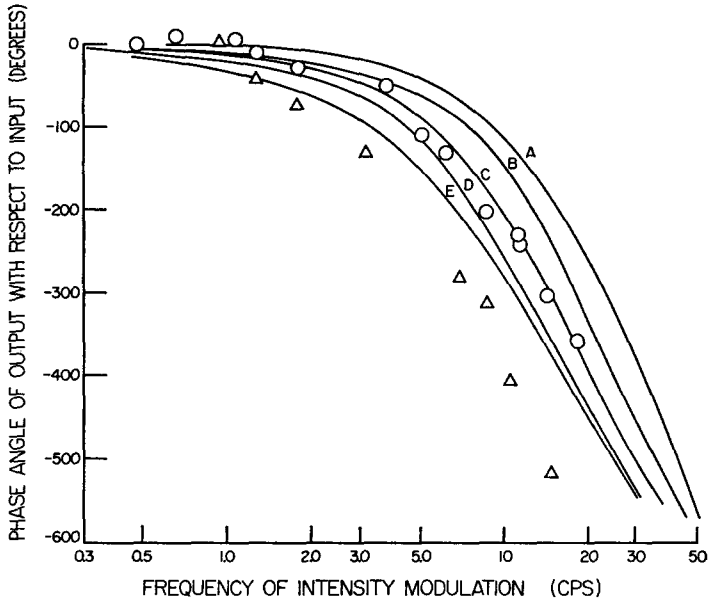

FIGURE 7. Comparison of phase angle characteristics of equation (1) with experimental results of Fig. 3. Solid curves *A*, *B*, *C*, *D*, and *E* are phase angles corresponding to small-signal amplitude characteristics of Fig. 6, and are phase angles of V_o with respect to V_1. ○, phase angle of generator potential with respect to intensity sinusoid, corresponding to same symbol for amplitude in Fig. 6. △, phase angle of generator potential with respect to intensity sinusoid, corresponding to same symbol in Fig. 6. Parameter values of equation (1), same as for Fig. 6.

any input with a nonzero mean level, but rather a cascade of RC elements with feedback loops from the output to each RC element.[2] For the case of a small amplitude input on a nonzero mean level, these feedback loops are linear, and undistorted sine waves are present in the output, for small input variations.

Since curves *E* and *D* of Fig. 6 correspond to low mean relative voltage levels, it might be said that this preparation is of low light sensitivity. However,

[2] An exception to this occurs at very high frequencies, see Appendix and Discussion.

in other preparations at even higher mean intensities than used here, amplitude peaking did not exceed that of curve *C* in Fig. 6.

It has been established that this model with 10 sections has responses to large steps of light which are qualitatively similar to those of the generator

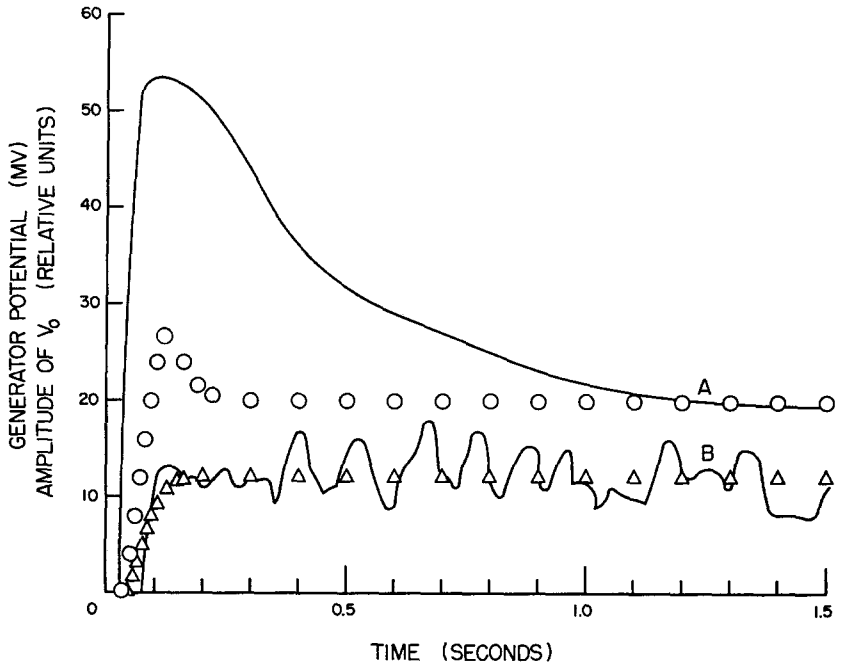

FIGURE 8. Comparison of step responses of generator potential with step responses o model, equation (1). Solid curve *A*, response of generator potential to a step from dark-adapted state, intensity of step 13,600 lumens/m², same value as mean intensity for circles of Figs. 6 and 7. **O**, response of V_0 (equation 1) to a step from zero of 0.11 v, same value as mean input for curve *D* (Fig. 6 and 7). Solid curve *B*, response of generator potential to a step from dark-adapted state, intensity of step 13.6 lumens/m², same value as mean intensity for triangles of Figs. 6 and 7. △, response of V_0 to a step from zero of 0.0001 v or less, where also $aV_0 \ll g_0$, as in curve *E* (Figs. 6 and 7). Parameters of model equation (1) are same as for Fig. 6. Model inputs start from zero so the model is initially dark-adapted. Generator potentials are measured relative to resting potential, and replotted from original recordings. Rapid variations or noise present on curve *B* are typical of low intensity level step responses. Experiment of 14 November 1963.

potential (Fuortes and Hodgkin, 1964, Fig. 13), and for 9 sections this simulation has demonstrated the same. A critical test of the model in this case is to compare its "dark-adapted" step responses with those of the dark-adapted photoreceptor for step voltage and intensity equal to the mean voltage and intensity in Figs. 6 and 7. This is shown in Fig. 8, and it is apparent that the qualitative agreement is present, since the overshoot for the higher step in-

tensity is greater than that for the lower step intensity. The step responses of the model have been scaled in magnitude so that the steady-state values are equal to those of the generator potential. However, the per cent peak overshoot of the generator potential is far greater than that of the model, and this constitutes a quantitative disagreement between model and these experimental results. Such disagreement is not apparent in the work of Fuortes and Hodgkin (Fig. 13, 1964) where the complete form of the step response was predicted from two aspects of the step responses of the dark-adapted eye. In the present work the step response has been predicted after finding model parameters for a good observed fit to experimental sinusoidal characteristics of the light-adapted eye.

The model, of course, does have step responses which have far greater overshoot, but these responses are much too oscillatory, and the corresponding sinusoidal responses are too peaked. This situation does not change for a limited increase or decrease in the number of sections. Attempts to make the feedback dependent on rate of change of V_o have not met with any success in closer simulation of step responses.

C. *Low Frequency Sinusoidal Stimuli*

Figs. 2 and 3 indicate that as frequency is decreased below 1 CPS the amplitude of the generator potential is decreasing and the phase angle of the generator potential is leading the stimulus. However, the model based on equation (1) predicts only constant amplitude response and zero phase angle as frequency decreases below 1 CPS. Apparently an additional dynamic element is required in the model to describe the low frequency behavior of the generator potential. Such an element which has the low frequency behavior shown by the generator potential is known as a "linear lead network," and is described by equations (2) and (3),

$$V_p = V_o - V_q \tag{2}$$

$$k\tau \frac{d}{dt} V_q + V_q = (1 - k)V_o \tag{3}$$

where V_o is the input to this dynamic element, V_p is the output, and V_q is an intermediate variable. Frequency response properties of this dynamic element are a zero frequency gain smaller than high frequency gain by a factor of k, $(k < 1)$ and a phase lead of V_p with respect to V_o over the range of frequency where gain is changing. The gain property is seen in the following manner: at zero frequency, $\frac{d}{dt} V_q = 0$, and combining equations (2) and (3), $V_p = kV_o$. At high frequency, $V_q \simeq 0$, and $V_p = V_o$. For the present, V_o, the output of equation (1), will be the input to equations (2) and (3).

The circles of Fig. 9 *A* and 9 *B* are the amplitude and phase characteristics of generator potential at frequencies of 1 CPS and below. It is then natural to examine also the time-dependent behavior of the generator potential to incremental long period waveforms other than sinusoids in order to discover

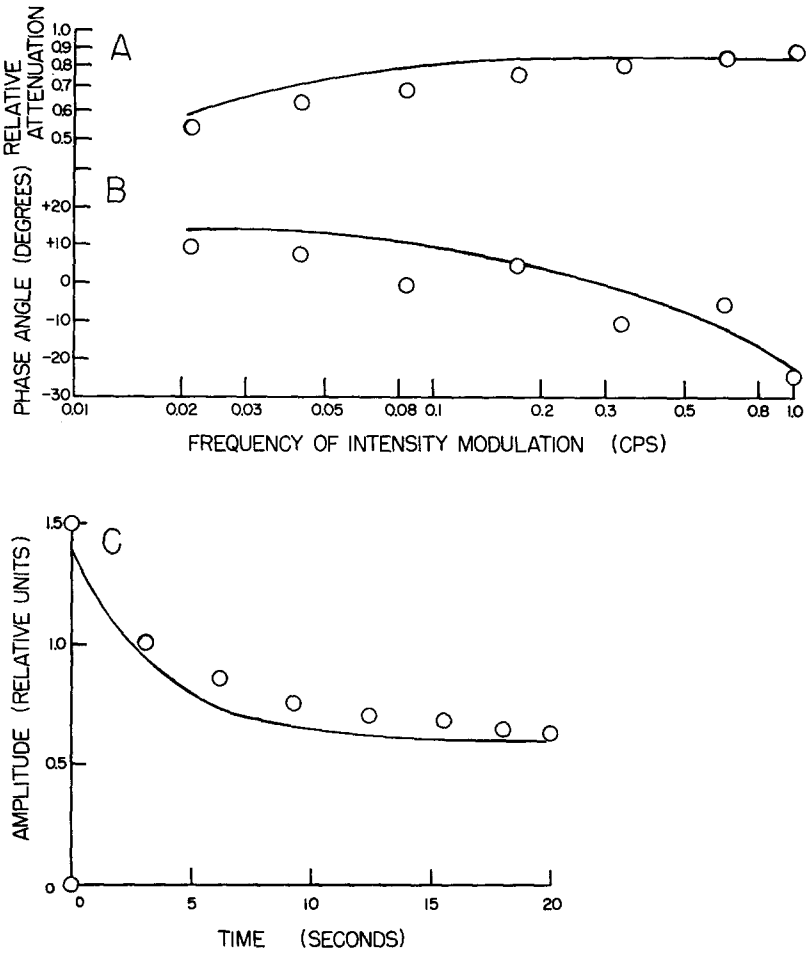

FIGURE 9. Low frequency incremental sinusoidal and step responses. *A*, **O**, amplitude characteristic of peak to peak generator potential, 9500 lumen/m² mean intensity, 30% sinusoidal modulation, experiment of 31 March 1964; solid curve, amplitude characteristic of V_p in response to incremental sinusoidal modulation of V_1, input to equation (1). *B*, phase angle characteristics for amplitudes in *A*. *C*, O, amplitude of one-half cycle of steady-state generator potential in response to +5700 lumen/m² incremental periodic square wave on 9500 lumen/m² mean level, light-adapted, experiment of 27 March 1964; solid curve, response of V_p to an incremental periodic square wave of V_1. Parameters in *A*, *B*, *C*, for equation (1) as in Fig. 6, curve *D*. Parameters in *A*, *B*, *C* for equation (3), $k = 0.6$, $\tau = 6$. Calculations of model responses in this case are made by usual operational and complex algebra methods.

whether or not equations (2) and (3) accurately describe the low frequency *and* long time behavior of the generator potential. An incremental long period periodic square wave of light intensity was applied to a preparation different from that of 9 *A* and *B*. The circles of Fig. 9 *C* show the relative amplitude of the steady-state generator potential during one-half cycle of the incremental square wave stimulation. It is noted that the decay from the peak of Fig. 9 *C* is considerably longer than the decay from the initial peak apparent in the step response of the dark-adapted eye (Fig. 8).

The parameters k and τ of equation (3) have been adjusted so that the complete model consisting of equations (1) (parameters as in curve *D*, Fig. 6), (2), and (3) fits the frequency and time data of Fig. 9 to a reasonable first approximation. Equation (1) influences only the phase angle down to approximately 0.3 CPS. The calculations of the complete model are shown as solid lines in Fig. 9, and demonstrate, to a first approximation, that the low frequency response of the generator potential is related to the long time behavior in that both are described by the same linear differential equations. This statement is equivalent to saying that the appropriate Fourier transform of the circles of Fig. 9 *C* would yield the frequency characteristic of Fig. 9 *A* and *B*. However, due to the limited number of data points, Fourier transforms were not used here.

The value of $k = 0.6$ found in the fit of Fig. 9 agrees approximately with the value of k which can be predicted from Fig. 4. Incremental gains at zero frequency (first derivative of static characteristic) are one-half the incremental gains at 1 CPS (a high frequency), and thus in Fig. 4, $k = 0.5$. The parameter τ of the model for any of the responses of Fig. 4 is at least equal to 6 (unpublished data of the author), so that 1 CPS can be considered in Fig. 4 as a high frequency.

It will be noted that for these parameters the effect of equations (2) and (3) on the results of equation (1) alone is negligible for frequencies greater than 0.8 CPS or times shorter than 0.5 sec.

D. *Approximate Delta Function Stimuli*

A necessary condition for the validity of the small signal sinusoidal frequency response description of the photoreceptor is that the frequency response be derivable from the delta function response of the photoreceptor by means of the Fourier series. Experimentally, a narrow square pulse of light intensity will approximate a delta function.

Some typical averaged responses of the generator potential to narrow square pulses of light intensity on a mean level of complete light adaptation are shown in Fig. 10. Fig. 10 *A* and *B* show the effect of reversing the polarity of the narrow square pulse. It is apparent that the peak magnitude and latency are approximately the same in the two cases, which implies that the photo-

receptor can be considered small signal linear, in the light-adapted state. However, there are some subtle differences upon close examination. In all cases examined, the peak of the response to the negative going square wave was slightly more rounded than that of the positive going one, which may indicate slightly higher frequency response in the positive going case. The

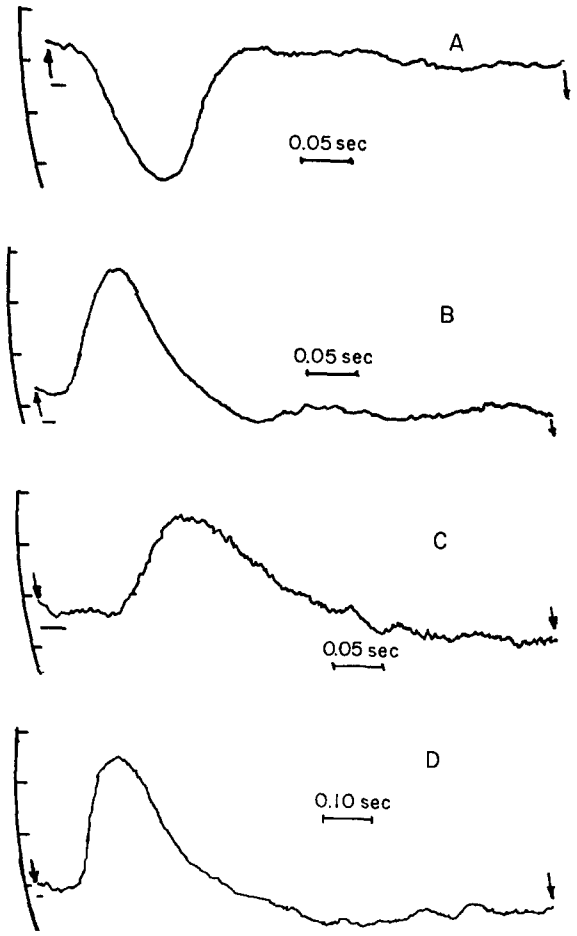

FIGURE 10. Averaged responses of generator potential to narrow square pulses of light superimposed on a mean level to which the photoreceptor is adapted. *A*, average of 601 responses to 12 msec, −5700 lumen/m² pulse on a 9500 lumen/m² mean level, ordinate 0.305 mv/div. *B*, average of 616 responses to 12 msec, +5700 lumen/m² pulse on a +9500 lumen/m² mean level, ordinate 0.296 mv/div. *C*, average of 600 responses to 22 msec, +57 lumen/m² pulse on a 95 lumen/m² mean level, ordinate 0.31 mv/div. *D*, average of 101 responses to 12 msec, +90 lumen/m² pulse on zero mean level, photoreceptor initially dark-adapted, ordinate 0.47 mv/div. On each record left-hand arrow indicates the start of the square pulse, and right-hand arrow indicates the end of averaging computer sweep. Line below left-hand arrow indicates length of square pulse. All experiments of 31 March 1964.

slight downward trend of both responses (Fig. 10 *A* and *B*) immediately after the beginning of the square pulse was proven to be an artifact due to capacitive coupling of the square pulse into the input channel of the averaging computer. This artifact was measured for the number of responses averaged in each case and removed before frequency analysis. The waveforms of Fig. 10 *C* and *D*, demonstrate the increase in latency and attenuation of high frequencies which occurs at lower mean intensity levels, which has been shown in one case by Fuortes and Hodgkin (Fig. 12, 1964).

Since action potentials which are decrementally conducted toward the electrode site may be present on the recorded generator potential, the approximate delta function of light intensity must have an area which is sufficiently small so that an action potential is not generated, since in determining the frequency content of the generator potential, the action potential would be an artifact. During the experiment the generator potential was monitored, and no responses with action potentials were used. The approximate delta function is the ideal alternate way of obtaining the frequency response of the generator potential since it possesses a small area, with a small probability of generating an action potential. Hyperpolarizing currents may be used, but they have the theoretical possibility of altering parameters of the dynamic system of the photoreceptor.

The Fourier series of a train of square stimulus pulses of amplitude E, width $2\pi k$, and period 2π is given by equation (4).

$$F(\theta) = \frac{2E}{\pi}\left(\sin \pi k \cos \theta + \frac{1}{2}\sin 2\pi k \cos 2\theta + \cdots\right) = \frac{2E}{\pi}\sum_{n=1}^{\infty}\frac{1}{n}\sin n\pi k \cos n\theta \tag{4}$$

Examination of this Fourier series will show that the train of pulses is an approximation to a train of delta functions centered about $\theta = 0, 2\pi, \cdots$ within 5% up to the harmonic for which $n\pi k = 0.60$, since $\sin n\pi k \simeq n\pi k$ in this range. The Fourier series of generator potential responses was taken by a computer program approximating the integrations of equations (5) and (6) by summations. The variables $a(n)$ and $b(n)$ are the Fourier coefficients.

$$a(n) = \frac{1}{\pi}\int_{o}^{2\pi} f(\theta) \cos n\theta \, d\theta \tag{5}$$

$$b(n) = \frac{1}{\pi}\int_{o}^{2\pi} f(\theta) \sin n\theta \, d\theta \tag{6}$$

This program was tested by taking Fourier series of square waves, delta functions, and other functions. Data inputs to the computer were punched

cards, and samples of the generator potential waveform were taken so that there were at least 10 samples per cycle of the highest harmonic present. The sampled length of the record of the response determined the period of the fundamental frequency examined. No artificial zeros were used in extending the period of the fundamental. The length of the sampled record of

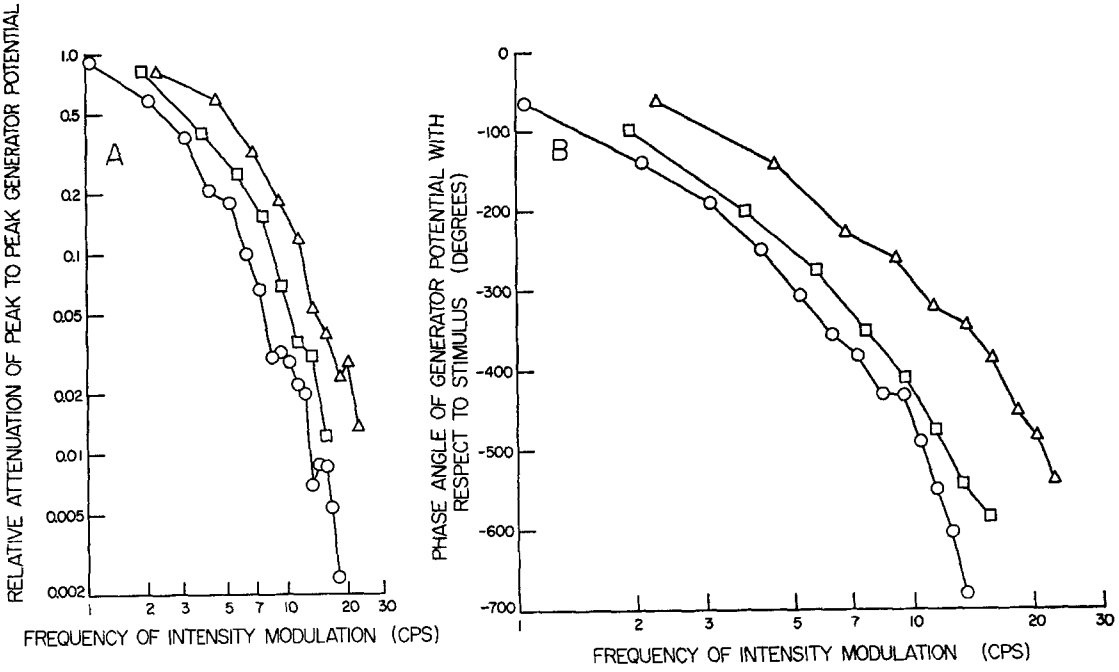

FIGURE 11. Incremental gain amplitude and phase characteristics of generator potential of light-adapted photoreceptor in response to a narrow square pulse of light (approximate delta function). Points are from incremental gain calculations on averaged responses (see text). A, B, △, amplitude and phase characteristics calculated from average of 365 responses to a +5700 lumen/m², 24 msec pulse on 9500 lumen/m² mean level. A, B, □, amplitude and phase characteristics calculated from average of 600 responses to +57 lumen/m², 24 msec pulse on a 95 lumen/m² mean level. A, B, ○, amplitude and phase characteristics calculated from average of 101 responses to +90 lumen/m², 10 msec pulse on a zero mean level. In each case the photoreceptor is adapted to the given mean level. Experiment of 31 March 1964.

the response was the length of the sweep of the averaging computer, and, in some cases, slightly less due to noise near the end of the response as obtained from the averaging computer.

The incremental gain of the photoreceptor is calculated from equations 4 to 6 in the following way. For the n^{th} harmonic, the output generator potential is equal to $\sqrt{a^2(n) + b^2(n)}$ mv peak at a phase angle $\angle \arctan \frac{-b(n)}{a(n)}$

relative to the input function $\left[\frac{2E\sin n\pi k}{\pi n}\right](\cos n\theta)$ lumen/m². Therefore, for this case

$$\text{Incremental gain} = \frac{\sqrt{a^2(n) + b^2(n)}}{\frac{2E}{\pi n}\sin n\pi k} \frac{\text{mv}}{\text{lumen/m}^2} \Big/ \arctan \frac{-b(n)}{a(n)}.$$

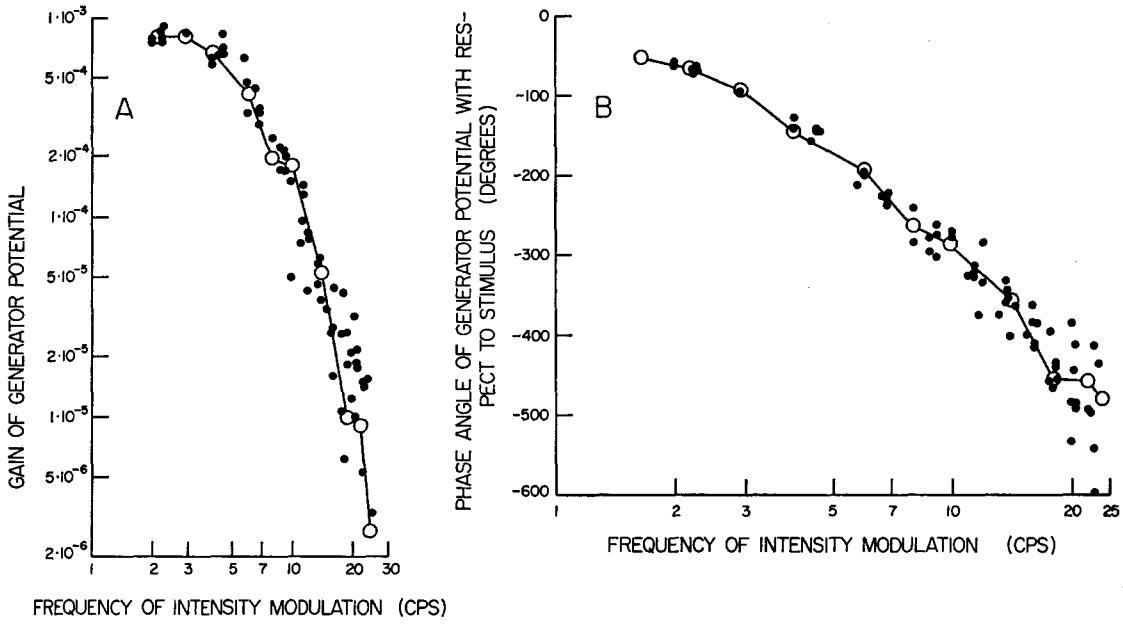

FIGURE 12. A, filled circles, gain (mv/lumen/m²) of photoreceptor calculated from ratio of peak frequency component of averaged generator potential response (in millivolts) to peak frequency component of stimulating pulse (in lumens/m²) (see text), all at same light-adapted mean level, 9500 lumens/m²; gain calculated for stimulus pulse amplitude and widths as follows: +2850 lumens/m², 12 msec; +5700, 24; −5700, 24; −5700, 12; +5700, 12; +2850, 12; −2850, 12; open circles, gain (mv/lumen/m²) of photoreceptor calculated for sinusoidal stimulation at 30% modulation, 9500 lumens/m² mean level. B, phase angles corresponding to gains of A. All experiments of 31 March 1964.

The incremental gains of a photoreceptor yielding responses such as those of Fig. 10 are shown in Fig. 11, where the amplitude curves are placed arbitrarily on the ordinate. Actually, the zero frequency gain of the lowest mean intensity curve is several orders of magnitude greater than that for the highest mean intensity, but the curves have been placed together to show their relative frequency content. It can be seen that the high frequency content varies as the mean intensity by examining the difference between the curves at 2

and at 8 CPS. This bears out the observation on the averages of the delta function response. A greater phase lag angle at lower mean intensity is shown in Fig. 11 *B*, which would be expected on examining Fig. 10.

In order to give a verification of the frequency response for stimuli other than sine waves, both the sinusoidal stimulus frequency response (averaged) and the frequency response as calculated from equations 4 to 6 were obtained

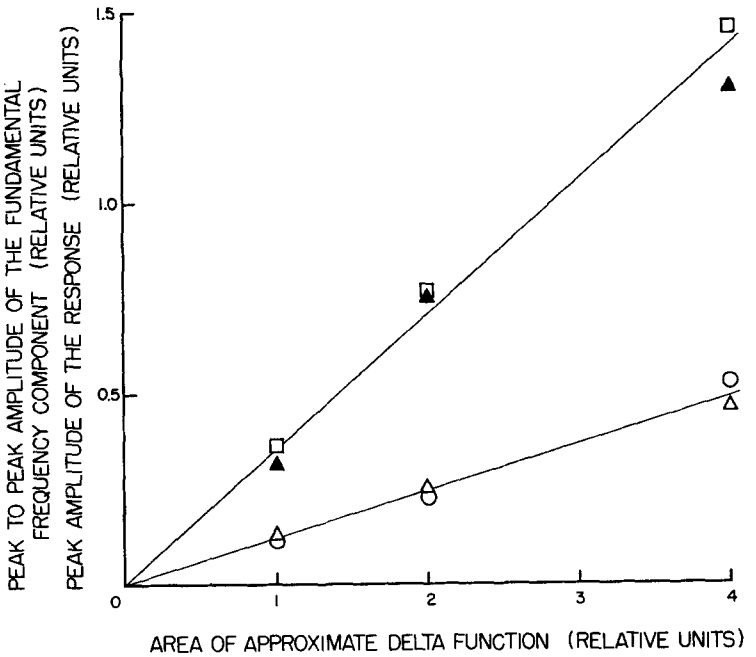

FIGURE 13. Linearity of generator potential response to narrow pulse, which is an approximate delta function. Solid lines fit by inspection, and must necessarily pass through 0, 0. ○, peak to peak amplitude of the fundamental frequency component of response to positive pulses of Fig. 12. △, peak to peak amplitude of the fundamental frequency component of response to negative going pulses of Fig. 12. □, peak amplitude of response to positive narrow pulses. ▲, peak amplitude of response to negative going narrow pulses (both of Fig. 12). Experiment of 31 March 1964.

in the same experiment. In each case the incremental gains were calculated, and the amplitude responses of Fig. 10 *A* and *B* are two of the seven averaged responses at the same mean intensity used in obtaining the Fourier components of Fig. 12 *A*. Comparisons of phase angle are shown in Fig. 12 *B*, and over-all agreement is good. It will be noted that the scatter of the points increases with frequency; this is probably a result of the fact that the signal to noise ratio of the generator potential decreases with increasing frequency. The reasons that more averages were not taken are that the preparation has only a limited "life," and that experimentally it appears that an average with an

indefinitely large number of samples does not necessarily converge to one mean value.

A basis for stating that the generator potential is "small signal linear" is shown in Fig. 13, where both the peak to peak amplitude of the fundamental frequency component and peak amplitude of the averaged response to the approximate delta function are plotted with respect to the area of the approximate delta function. In linear system theory, the weight or area of the delta function is the pertinent parameter, and since the width of these light pulses (maximum 24 msec) was well within the limit for time-amplitude reciprocity, area is the pertinent parameter in this case. The points can be extrapolated reasonably well to (0, 0) which is necessary for linearity in this case. It should be noted that both scales of this plot are in effect absolute value scales.

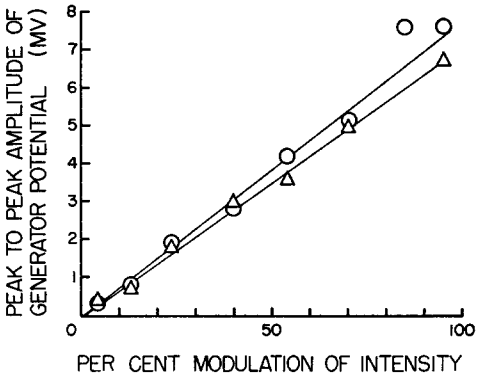

FIGURE 14. Dependence of generator potential amplitude on percentage sinusoidal modulation, at one mean intensity, 13,600 lumens/m^2. O, amplitude of generator potential at 1 CPS. △, amplitude of generator potential at 6 CPS. Experiment of 14 November 1963.

A somewhat surprising result regarding linearity of the generator potential is the extent of the linearity for sinusoidal incremental stimuli. A typical result for one mean intensity is shown in Fig. 14. Linearity holds to a reasonably large percentage modulation. This was true for all preparations and all mean intensities examined. Linearity with respect to per cent modulation is also shown by the circles of Fig. 4.

DISCUSSION

One object of these experiments has been to examine the dependence of the dynamics of the photoreceptor of *Limulus* upon the mean intensity of light to which the photoreceptor is adapted. It is apparent that the frequency response of the photoreceptor reflects some aspects of the large signal step response in its change of amplitude and phase characteristic with respect to mean intensity. However, in general, a nonlinear system will possess large-signal behavior which cannot be derived from small-signal or incremental behavior, and in *Limulus* there is no unique way of connecting these two states

or modes of behavior. The large-signal step response from the dark-adapted state and incremental responses may be further differentiated on the basis of the photoreceptor being in two separate states, dark and light adaptation. This may further complicate the nonlinearities.

One means of unifying the large- and small-signal behavior is a model based on the absorption of light and molecular kinetics of rhodopsin related to the change of membrane resistance and depolarization of the eccentric cell. But insufficient knowledge is available for such a model directly deduced from molecular theory, and a mathematical basis has been formed instead. Eventual molecular models must, of course, have mathematical properties similar to those found by Fuortes and Hodgkin (1964) and those found in these experiments. Both the model of Fuortes and Hodgkin (1964) and the model proposed by the author (Jones, Green, and Pinter, 1962) do relate in one respect to molecular models, in that they both describe chemical kinetics involving autocatalysis; i.e., a product affects the rate constants of its own formation.

The model proposed by the author (Jones, Green, and Pinter, 1962) (with added linear elements to increase phase lag and attenuation) possesses large step and frequency response properties of the *Limulus* photoreceptor, but does not give the proper reciprocity relation for short input pulses, due to the presence of an algebraic logarithmic function preceding the dynamics. However, a case can be made for an algebraic logarithmic function not existing subsequent to the dynamics, for sinusoidal light intensity modulation. The distortion (Fig. 1 *F*) present on the generator potential for large percentage modulation at low frequencies (1 CPS and below) disappears as frequency is raised (to 5 CPS and above) even though peak to peak generator potential does not change by a large amount (Fig. 2). If some of this distortion (assuming it is not vanishingly small) were caused by an algebraic logarithmic element subsequent to the dynamics, such distortion would not disappear as frequency is raised, until, of course, the peak to peak excursions of the generator potential or transmitter substance concentration became very small.

In examining the comparison of sinusoidal amplitude data from *Limulus* with the model (Fig. 6), one might ask whether or not a mean intensity higher than in these experiments would produce greater amplitude peaking, as is shown by the model for larger mean inputs (curve *A*, Fig. 6). However, the mean intensities used in these experiments are approximately only one logarithmic unit (to base 10) less than full skylight plus sunlight. Considering the usual environment of *Limulus*, these intensities are physiological at the surface of the cornea. Successful preparations almost invariably had clear corneas. In one early experiment, the stimulator was arranged to yield a mean intensity of 136,000 lumens/m^2 at the surface of the cornea, and amplitude peaking of the frequency response was only slightly higher than in Fig. 2.

Comparison of the large-signal step responses of *Limulus* with the RC nonlinear model of Fuortes and Hodgkin (1964) reveals certain quantitative deficiencies (Fig. 8). Fuortes and Hodgkin (1964) found that the response predicted by the model to large steps from the dark was too oscillatory, when their model parameters were fixed by means of calculations from the initial rise and steady-state values of the step response. On the other hand, the model parameters were found in the present work by an observed fit to light-adapted sinusoidal frequency response, and from this a prediction of large-signal dark-adapted step response was attempted. The primary deficiency of the model in this case is one of insufficient initial peak amplitude in the dark-adapted step response. This suggests that an additional rate-sensitive dynamic element which affects neither the initial slope nor the steady-state value of the model output is required in combination with the RC nonlinear model and equations 2 and 3. This rate-sensitive element would necessarily depend on the state of dark or light adaptation, since the element would affect the step response of only the dark-adapted eye.

The highly oscillatory model step responses of Fig. 13 of Fuortes and Hodgkin (1964) would predict sharply peaked amplitude frequency response characteristics of the photoreceptor for mean intensities of the same values as the steps, since these two properties occur together in this model. If the large-signal step response of equation (1) is highly oscillatory, the natural frequency is relatively undamped, giving rise to amplitude frequency peaking. The present work suggests that if the frequency response had been measured for the preparation of Fig. 13 of Fuortes and Hodgkin (1964), the amplitude peaking would not approach that of the model for the given parameters.

Other quantitative deficiencies appeared in the complete model responses (equations 1 to 3). For sinusoidal inputs of 95% modulation near 0.5 CPS the model exhibits a double peaking in the output waveform and in the limit as frequency is decreased (at 95% modulation) a log sine response appears (unpublished data of the author). Neither of these properties is found in the generator potential (see Fig. 1 *F*). The response of the complete model to the "off" of the step of light from the dark is a fast monotonic decay to the original resting value, zero (unpublished data of the author). However, subsequent to the off of the step the generator potential decays rapidly at first to a value more positive than the original resting value, and then very slowly to the original resting value (Fuortes and Hodgkin, 1964; Benolken, 1959). Further, during the slow decay there is a concomitant slow increase in absolute gain (Stevens, 1964). Define absolute gain as the ratio of peak generator potential response to stimulating pulse intensity with zero background intensity. It can be said that if the complete model possessed the slow decay property, it would also show the slow increase in absolute gain by virtue of its output-dependent property.

Placing the low frequency section of the complete model (equations 2 and 3) subsequent to the RC nonlinear networks (equation 1) is not an arbitrary choice. This configuration permits the statement to be made under Results (section C) that the low frequency section does not modify the high frequency behavior of equation (1). Further, if the low frequency behavior shown in Fig. 9 can be considered a neural adaptation, it appears that the model section simulating the neural adaptation should be near the output or neural end of the complete model. Underlying this statement is the assumption that the RC nonlinear networks correspond to the initial stages of photoreception.

Whenever long period incremental stimuli are used, such as in Fig. 9 *C*, a question may arise as to whether or not the response obtained is caused in part by a variation in the degree of light adaptation. However, the time constant of the square wave generator potential response of Fig. 9 *C* is approximately 3.6 sec, much too small to be caused by variations in rhodopsin concentration (Campbell and Rushton, 1955, Fig. 3).

There is a large difference between the neural adaptation in the light-adapted state (Fig. 9 *C*), and the decay of the generator potential from the initial peak of the dark-adapted step response (Fig. 8). It is difficult to relate these two types of decay since they occur in different time scales, and, most important, in different states of adaptation. Further, the decay from the initial peak can be thought of as a property of the high frequency dynamics of the photoreceptor and the slow decay a property of the low frequency dynamics of the photoreceptor.

In Fig. 13 linearity for incremental pulse responses has been shown for pulse amplitudes to 60% modulation (pulse amplitudes, Fig. 12), but only one mean intensity level. From Fig. 14, linearity of sinusoidal response holds to at least 60% modulation. Linearity of pulse responses for lower mean intensities might be expected in view of linearity for incremental sinusoidal stimuli at lower mean intensities (circles of Fig. 4). It might also be expected that the equivalence in Fig. 12 would hold for lower mean intensities, but these points remain to be tested.

In Fig. 14 it should be noted that distortion present in the generator potential at 85 and 95% modulation (see Fig. 1 *F*) has been included in the peak to peak measurement. This distortion is present at 1 CPS but not at 6 CPS, and causes slightly higher amplitude points on the graph of Fig. 14 for 85 and 95% modulation at 1 CPS. This distortion is removed by the dynamics of the photoreceptor as frequency is raised, in the same manner that a similar distortion in the model response is removed by the model dynamics as frequency is raised (equations 1 to 3 and 95% modulation). However, the distortion in the generator potential at very low frequencies, below 0.2 CPS, is not related to its steady-state logarithmic characteristic, i.e., there is no log sine response

for 95% modulation. The state of light adaptation apparently removes the logarithmic characteristic, but this does not occur in the RC nonlinear networks. The distortion in Fig. 1 *F* may be related in one way to the dark-adapted step response. The dark-adapted step response of the photoreceptor shows a greater absolute value of time rate of change at the on of the step than at the off of the step (Fuortes and Hodgkin, 1964, Fig. 13). From this one might predict that the dynamic distortion (i.e., excluding that which might be caused by the steady-state logarithmic characteristic) at high percentage modulations would have a greater absolute value of rate of change during the rising portion of the stimulus than during the falling portion, and this occurs in Fig. 1 *F*.

It is interesting to note that the decrease of distortion with increase in frequency at 95% modulation in the model is easily explained in terms of the amplitude attenuation of the RC nonlinear networks. As frequency is raised (e.g., above 10 CPS for curve *D*, Fig. 6), the peak to peak variations in the term aV_o of equation (1) approach zero, making $(g_o + aV_o)$ a constant coefficient. Thus the RC nonlinear networks become linear at high frequencies, yielding undistorted sinusoidal outputs even at 95% modulation of the input.

There exists a means of proving that the latency apparent in the step response is a true transport lag or time delay rather than explaining in terms of the RC transmission line (or lumped approximation) delay property, which is due to products of exponential and power functions of time. This means could be achieved by measuring the phase angle of the generator potential at stimulus frequencies far higher than those examined here (50 CPS and beyond). If the latency is a true time delay, the phase lag angle continues to increase directly with frequency indefinitely. If the latency is explained in terms of the RC line properties, the phase lag angle has a limit which is 810° for the 9 section RC model, or $n \cdot 90°$ for an n section model. For Fig. 7, this limit would be reached at approximately 150 CPS. Unfortunately, the signal to noise ratio and possible nonstationarity, combined with the limited life of this preparation seem to preclude making measurements even approaching this frequency.

A certain similarity exists between the sinusoidal amplitude characteristics in Fig. 2 and the amplitude frequency attenuation characteristics measured on the human visual system by subjective threshold (DeLange, 1957; and Kelly, 1961 *b*). For a linear system, a threshold measurement is equivalent to measuring an input-output ratio, but the linearity of the human visual system cannot be guaranteed even for small signals. Nevertheless, it is interesting to note that the human visual attenuation characteristics possess a peak which diminishes as mean intensity (to which the subject is adapted) is decreased, in a manner similar to Fig. 2. However, this peak has a greater relative amplitude and occurs at a higher frequency than does that of *Limulus*. This might reflect the difference in temperature in the two processes. Prelimi-

nary results of sinusoidal amplitude frequency response experiments on the retinal ganglion cell of the cat have also shown peaking at approximately 8 CPS (Enroth and Cleland, 1964), suggesting that the mechanism behind frequency response peaking for higher animals lies within the retina.

Appendix

The small-signal incremental behavior of equation (1) is given by the small-signal linearization of equation (1). Assume that

$$V_i = \bar{V}_i + v_i$$

$$V_o = \bar{V}_o + v_o$$

where $\bar{V}_i$, $\bar{V}_o$ are constant components, and v_i, v_o are small variations about the constants. In other words, the variables are broken down into constant and small variation components. Now substitute these variables into equation (1), and simplify the expression

$$\frac{dv_i}{dt} = \frac{\bar{V}_{i-1} + v_{i-1}}{C} - \frac{g_o}{C}[\bar{V}_i + v_i] - \frac{a}{C}[\bar{V}_i \bar{V}_o + \bar{V}_i v_o + \bar{V}_o v_i + v_o v_i]$$

Assume now that v_i and v_o are sufficiently small so that $v_o v_i \simeq 0$. Then the resulting equation is linear.

$$\frac{dv_i}{dt} = \frac{\bar{V}_{i-1} - g_o \bar{V}_i - a\bar{V}_i \bar{V}_o}{C} + \frac{v_{i-1}}{C} - v_i\left(\frac{g_o + a\bar{V}_o}{C}\right) - v_o\left(\frac{a\bar{V}_i}{C}\right)$$

When the steady state to the mean input is reached, it is true that

$$\frac{\bar{V}_{i-1} - g_o \bar{V}_i - a\bar{V}_i \bar{V}_o}{C} = 0,$$

and the equation becomes

$$\frac{dv_i}{dt} = \frac{v_{i-1}}{C} - v_i\left(\frac{g_o + a\bar{V}_o}{C}\right) - v_o\left(\frac{a\bar{V}_i}{C}\right),$$

which is a linear equation describing an RC network, but with negative, linear feedback from the output in the term $v_o\left(\frac{a\bar{V}_i}{C}\right)$. Such a system has the possibility of amplitude frequency peaking.

Note that at very high frequencies, due to attenuation in each RC network, $v_o \simeq 0$, and the equations in this case do appear as those of a simple cascade of RC elements.

The author wishes to thank Professor Richard W. Jones for continuing interest and guidance during the course of this work. Gratitude is extended to Drs. R. M. Benolken, Leo L. Lipetz, Christina Enroth-Cugell, and H. K. Hartline for particularly helpful discussions.

This work was supported in part by research grant B-2165 from the Council on Neurological Diseases and Blindness, National Institutes of Health, Public Health Service, R. W. Jones, principal investigator.

Received for publication 21 April 1965.

BIBLIOGRAPHY

BENOLKEN, R. M., 1959, Ph.D. Dissertation, The Johns Hopkins University, Baltimore.

CAMPBELL, F. W., and RUSHTON, W. A. H., 1955, *J. Physiol.*, **130,** 131.

CLYNES, M., 1961, *Ann. New York Acad. Sc.*, **92,** 946.

DELANGE, H., 1957, Ph.D. Dissertation, The Technical University of Delft, Delft, Holland.

ENROTH, C. E., and CLELAND, B., unpublished experimental observations, 1964.

FUORTES, M. G. F., 1958, *Am. J. Ophth.*, **46,** 210.

FUORTES, M. G. F., and HODGKIN, A. L., 1964, *J. Physiol.*, **172,** 239.

FUORTES, M. G. F., AND POGGIO, G. F., 1963, *J. Gen. Physiol.*, **46,** 435.

GEISLER, C. D., Technical Report No. 280, Massachusetts Institute of Technology Research Laboratory of Electronics, Cambridge, Massachusetts, 1960.

HARTLINE, H. K., 1935, *Cold Spring Harbor Symp. Quant. Biol.*, **3,** 245.

JONES, R. W., GREEN, D. G., AND PINTER, R. B., 1962, *Fed. Proc.*, **21,** 97.

KELLY, D. H., 1961 *a*, *Rev. Scient. Instr.*, **32,** 50.

KELLY, D. H., 1961 *b*, *J. Opt. Soc. America*, **51,** 422.

MACNICHOL, E. F., JR., 1956, *in* Molecular Structure and Functional Activity of Nerve Cells, (R. G. Grennell and L. J. Mullins, editors), Washington, American Institute of Biological Sciences, 34.

RATLIFF, F., HARTLINE, H. K., and MILLER, W. H., 1963, *J. Opt. Soc. America*, **53,** 110.

STEVENS, C. F., unpublished experimental observations, 1964.